Constraints on box-shaped cosmic ray electron feature from dark matter annihilation with the AMS-02 and DAMPE data

Lei Zu,[1,2] Cun Zhang,[1,3] Lei Feng,[1,*] Qiang Yuan,[1,2,†] and Yi-Zhong Fan[1,2,‡]

[1]*Key Laboratory of Dark Matter and Space Astronomy, Purple Mountain Observatory, Chinese Academy of Sciences, Nanjing 210008, China*

[2]*School of Astronomy and Space Science, University of Science and Technology of China, Hefei 230026, Anhui, China*

[3]*School of Physics, Nanjing University, Nanjing, 210092, China*

Abstract

Precise measurements of spectra of cosmic ray electrons/positrons can effectively probe the nature of dark matter (DM) particles. In a class of models that DM particles first annihilate into a pair of intermediate particles which then decay into standard model particles, box-shaped spectra can be produced. Such energy spectra of cosmic rays are distinct from astrophysical backgrounds, and can probably be regarded as characteristic features of the DM annihilation. In this work, we search for such spectral feature in the total electron plus positron fluxes by AMS-02 and DAMPE. We find no significant signal of the DM annihilation into box-shaped electrons/positrons. The 95% confidence level upper limits of the velocity-weighted cross section are derived, which range from $\sim 10^{-26}$ cm^3 s^{-1} for DM mass of 50 GeV to $\sim 10^{-24}$ cm^3 s^{-1} for DM mass of 10 TeV.

PACS numbers: 11.15.Kc

*Electronic address: fenglei@pmo.ac.cn

†Electronic address: yuanq@pmo.ac.cn

‡Electronic address: yzfan@pmo.ac.cn

I. INTRODUCTION

Dark Matter (DM) is a very important concept in physics and astrophysics. Several methods were proposed to detect a kind of weakly interacting massive particle which is one of the most popular DM candidates, including the collider detection [1, 2], direct detection [3, 4], and indirect detection [5, 6]. The indirect detection of DM particles is to search for unexpected "excess" in the energy spectra of cosmic rays or γ-rays [11–14]. Recent progresses include the significant excesses of positron fraction and spectrum observed by PAMELA [15] and AMS-02 [16, 17], and the total electron plus positron spectra observed by ATIC [18], Fermi-LAT [8], and also AMS-02 [19], when compared with the predictions of cosmic ray propagation model. The model prediction of antiproton fluxes is largely consistent with the data [20–22] (see, however, [23, 24]).

Either the DM annihilation/decay models [25–34] or astrophysical sources [35–42] have been proposed to interpret the electron and positron excesses. For DM annihilation models, the annihilation cross section needs to be about 10^{-23} cm^{3}s^{-1} which is too large to give the correct (observed) relic density and a large boost factor ($\sim 10^3$) is needed [27, 43]. For DM decay models, the lifetime of DM is about 10^{26} s. Such models have been stringently constrained by observations of γ-rays [44–46], radio emission [47, 48], and the cosmic macrowave background (CMB; [49, 50]).

In this work, we focus on the scenario that DM particles annihilate/decay into a pair of intermediate particles which then decay into Standard Model particles [51, 52]. It can also produce box-shaped spectrum to get distinguished from other astrophysical process efficiently. This model has been used to explain the antiproton data of AMS-02 [53]. The box-shaped γ-ray feature was searched with the Fermi-LAT data and constraints were reported [54, 55]. In this work, we search for such spectral feature in the total electron plus positron fluxes by AMS-02 and DArk Matter Particle Explorer (DAMPE) [56]. The mass ratio of the intermediate particle and DM has been taken as a free parameter (if only the mass ratio can lead to a box-shaped spectrum). DAMPE is a new cosmic ray telescope with very high energy resolution (better than 1.5%@1TeV for electrons and γ-rays) and excellent hadron rejection power (higher than 10^5) [57, 58]. Such improvements are very helpful in identifying the unique structure of cosmic-ray spectrum and the measurements are expected to be able to tightly constrain the theoretical models. Recently, the DAMPE collaboration

has published their first result, i.e., the electron plus positron spectrum [56]. The DAMPE data cover the energy range from 25 GeV to 4.6 TeV, which provides us a good probe of the properties of DM particles.

This work is organized as follows: In Section II, we describe the energy spectrum of electrons and positrons generated by the DM two-step cascade annihilation. In Section III A, we explore such feature in the AMS-02 and DAMPE data and derive the constrains on the parameter space. Then we focus on the local subhalo scenario with box-shaped spectrum in Section III B. Our conclusions are summarized in Section IV.

II. BOX SHAPED SPECTRA

We focus on the two-step annihilation where DM annihilates into a pair of scalar particles ϕ which then decay into electrons and positrons. In the rest frame of ϕ, the energy of the final electron and positron is $E_{e^\pm} = m_\phi/2$. Since we focus on high energy cosmic rays, it is reasonable to assume that $m_e \ll m_\phi < m_{\rm DM}$ where $m_{\rm DM}$ is the mass of DM particles. If the mass of ϕ is comparable with $m_{\rm DM}$ or $2m_e$, a narrow peak spectrum can be generated [53]. In the lab frame, where the DM particles are non-relativistic and $E_\phi = m_{\rm DM}$, the energy of the final electron/positron is

$$E = \frac{m_\phi^2 + \beta\cos\theta\sqrt{4m_{\rm DM}^2 m_e^2\left(\beta^2\cos^2\theta - 1\right) + m_\phi^4}}{2m_{\rm DM}\left(1-\beta^2\cos^2\theta\right)}, \tag{1}$$

where $\beta = \sqrt{1 - m_\phi^2/m_{\rm DM}^2}$, θ is the angle between the outgoing electron/positron and the parent scalar in the lab frame. To get the real solution(box-shaped SED), we let $m_\phi^2 > 2m_{\rm DM}m_e$ and then $m_\phi/m_{\rm DM} > \sqrt{1.022\times10^{-3}\ {\rm GeV}/m_{\rm DM}}$. Here we just consider the situation that $m_\phi/m_{\rm DM} = \{0.1, 0.5, 0.9\}$ and it is reasonable because $m_\phi/m_{\rm DM} > 0.001$ for $m_{\rm DM} = 1$ TeV and $m_\phi/m_{\rm DM} > 0.01$ for $m_{\rm DM} = 10$ GeV. From the above equation we see that the highest (lowest) energy corresponds to $\theta = 0^\circ$ ($\theta = 180^\circ$). Since the intermediator particle is a scalar particle, the distribution of outgoing angle of electrons/positrons in its rest frame is isotropic. Therefore the spectrum of the final electrons/positrons in the lab frame is a box-shaped spectrum in an allowed energy range

$$\frac{dN}{dE} = \frac{2}{\sqrt{\left(m_{\rm DM}^2 - m_\phi^2\right)\left(1 - 4m_e^2/m_\phi^2\right)}}\,\Theta(E - E_-)\,\Theta(E_+ - E), \tag{2}$$

where Θ is Heaviside function and $E_\pm = m_{\rm DM}/2 \pm \sqrt{\left(m_{\rm DM}^2 - m_\phi^2\right)\left(m_\phi^2 - 4m_e^2\right)}/2m_\phi$. We get the same result as that in Refs. [51, 52] if we set $dN/dE_{\rm rest} = \delta(E_{\rm rest} - m_\phi/2)$ in rest intermediator frame. And if $m_e = 0$, it returns to the photon emission spectrum [54]. Note that here we neglect the contribution of electroweak corrections. In Ref. [59], the authors calculated such processes in detail using the Pythia package [60], assuming a light intermediate particle. We will compare our results with that (labelled as "PPPC4") in the following.

From Eq. (2), we can see that there are two free parameters ($m_{\rm DM}$ and m_ϕ) to determine the spectrum. In the following discussion, we use $m_{\rm DM}$ and the mass ratio $m_\phi/m_{\rm DM}$ to present the results. If $m_\phi/m_{\rm DM} \sim 1$, it degenerates to the line spectrum. On the other hand, if $m_\phi/m_{\rm DM} \ll 1$ (but still $m_e \ll m_\phi$), the produced box-shaped spectrum is very broad. Fig. 1 shows illustrations of the energy spectra of electrons for $m_{\rm DM} = 1$ TeV and mass ratios of 0.1, 0.5, and 0.9. The result from PPPC4 is also presented in Fig. 1. We see clearly the effect on the broadening of the energy spectrum as the mass ratio decreases.

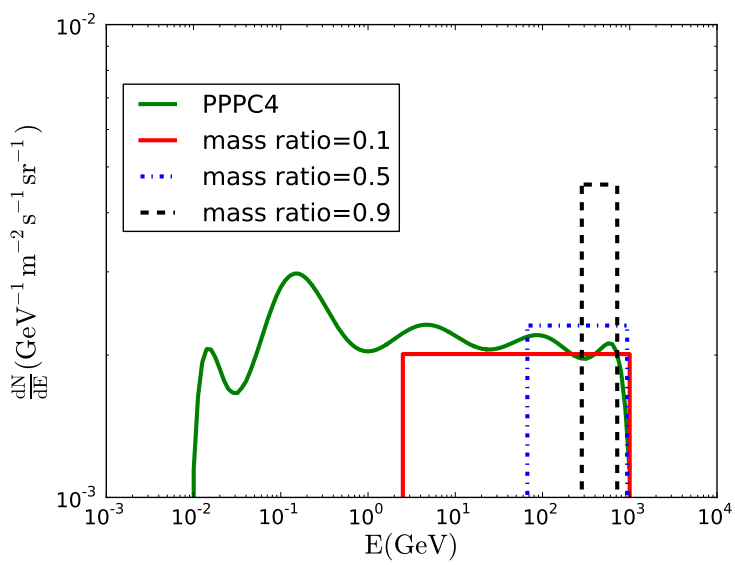

FIG. 1: The differential energy spectrum of electrons/positrons for different mass ratios between m_ϕ and $m_{\rm DM}$ and the PPPC4 (green line).

III. RESULTS

A. The smooth dark matter distribution scenario

To compare with the observational data, we also need to calculate the propagation of electrons/positrons in the Galaxy. There are some numerical codes developed to compute the propagation of cosmic rays, such as GALPROP [61] and DRAGON [62]. Here we adopt the LikeDM package [63], which employs a Green's function method (i.e., with quasi-monochromatic injection spectrum at a series of energy grids) to deal with the propagation of cosmic rays based on numerical tables obtained with GALPROP for given source spatial distribution, to calculate the propagation of electrons/positrons and the corresponding likelihood (or χ^2). There are several sets of density profiles of DM and propagation parameters in LikeDM. In this study we adopt the isothermal profile [64], and the propagation parameters with halo height of 4 kpc. See Ref. [63] for more details of the parameters.

The background includes the conventional primary electrons from e.g., supernova remnants, secondary electrons and positrons from the inelastic collisions between cosmic ray nuclei and the interstellar medium. Both components are phenomenologically described with broken power-law functions. For the primary electron spectrum, an additional cutoff is applied according to the DAMPE data [56]. A primary source of electron/positron pair from e.g., pulsars, is further assumed to account for the electron/positron excesses. This is because the DM interpretations of such excesses are strongly disfavored by the γ-ray and CMB observations [44–46, 49, 50]. The fluxes of the background electrons and positrons are described as [63]

$$\phi_{e^-} = C_{e^-} E^{-\gamma_1^{e^-}} \left[1 + \left(E/E_{\rm br}^{e^-} \right)^{\gamma_2^{e^-}} \right]^{-1} \exp\left(-E/E_c^{e^-} \right), \tag{3}$$

$$\phi_{e^+} = C_{e^+} E^{-\gamma_1^{e^+}} \left[1 + \left(E/E_{\rm br}^{e^+} \right)^{\gamma_2^{e^+}} \right]^{-1}. \tag{4}$$

The spectrum of the extra source is assumed to be an exponential cutoff power law

$$\phi_{\rm s} = C_{\rm s} E^{-\gamma^s} \exp\left(-E/E_{\rm c}^{\rm s} \right). \tag{5}$$

The total background energy spectrum of $e^- + e^+$ is then

$$\phi_{{\rm bkg},e^\pm} = \phi_{e^-} + 1.6\phi_{e^+} + 2\phi_{\rm s}. \tag{6}$$

In the second term of the right hand side, $0.6\phi_{e^+}$ represents the secondary electrons which are less than secondary positrons due to the charge conservation of the neutron production process [65].

The data used include the AMS-02 positron fraction [16], the AMS-02 $e^- + e^+$ fluxes in the range of 0.5 GeV $\sim$ 25 GeV [19], and the DAMPE $e^- + e^+$ fluxes [56]. The best-fit parameters of the backgrounds are given in Table I. Note that they are somewhat different from that given in Ref. [63] because of different data sets used in the fitting.

TABLE I: Best-fit parameters of the backgrounds

	C ($\mathrm{GeV^{-1}m^{-2}s^{-1}sr^{-1}}$)	γ_1	γ_2	E_{br} (GeV)	E_c (GeV)
ϕ_{e^-}	21.3417	0.8380	2.4075	3.3391	1.4435×10^4
ϕ_{e^+}	1.1947	0.7138	2.5898	2.7479	...
ϕ_s	0.9799	2.3828	...	...	842.93

When the DM contribution is added in the model, we enable the backgrounds to vary to some degree through multiplying adjustment factors $\alpha_i E^{\beta_i}$, with $i = \{e^-, e^+, s\}$, on ϕ_e^-, ϕ_e^+, and ϕ_{s}, respectively. The parameters α_i and β_i are optimized using the profile likelihood method. We scan the m_{DM} and $\langle\sigma v\rangle$ parameter plane of DM. If no signal is found, the 95% upper limits of the annihilation cross section for each DM mass m_{DM} is given by the condition that $\chi^2(\langle\sigma v\rangle) \leq \chi^2_{\mathrm{min}} + 2.71$. The 1-dimensional upper limits on the cross section and 2-dimensional likelihood maps on the $m_{\mathrm{DM}} - \langle\sigma v\rangle$ plane for several values of the mass ratio and for the energy spectrum given by PPPC4 code are shown in Figs. 2 and 3.

The 95% upper limits of the DM annihilation cross section range from $\sim 10^{-26}$ cm^3/s at $m_{\mathrm{DM}} = 50$ GeV to $\sim 10^{-24}$ cm^3/s at $m_{\mathrm{DM}} = 10$ TeV. The upper limits for different mass ratios do not differ much from each other. For $m_\phi/m_{\mathrm{DM}} = 0.9$ the results are slightly lower than the others. We find that the upper limits of $\langle\sigma v\rangle$ become weaker for $m_{\mathrm{DM}} \sim 2$ TeV. From Fig. 3 we can see that adding the DM component for $m_{\mathrm{DM}} \sim 2$ TeV can improve the fit to the data slightly. The test statistic (TS) value of such a DM signal is about 2.8. We show in Fig. 4 the comparison between the best-fit model and the data, for $m_{\mathrm{DM}} = 1.96$ TeV, $\langle\sigma v\rangle = 1.32 \times 10^{-24}$ cm^3/s, and $m_\phi/m_{\mathrm{DM}} = 0.9$. The DM contribution can slightly improve the match with the small bump of the DAMPE data around 700 GeV. However,

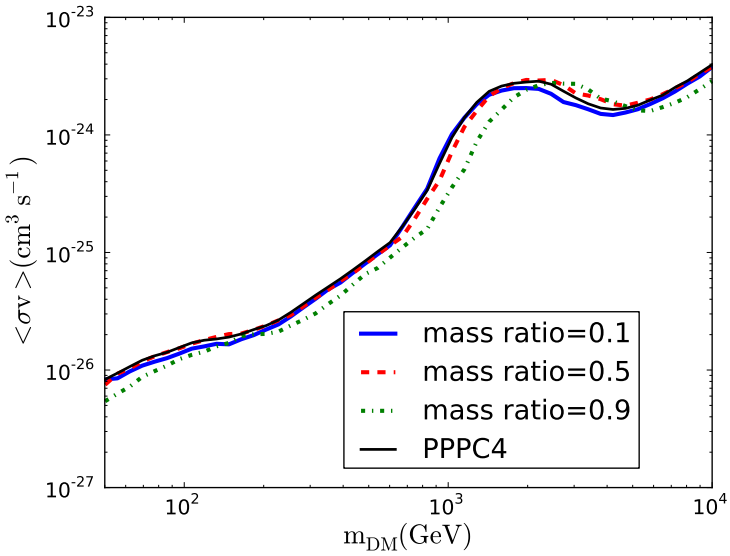

FIG. 2: The 95% confidence level upper limits on the DM annihilation cross section $\langle\sigma v\rangle$ as functions of $m_{\rm DM}$, for box-shaped spectra with $m_\phi/m_{\rm DM} = 0.1$, 0.5, 0.9, and the PPPC4 spectrum.

the significance is too small for the current data.

B. Local DM subhalo scenario

Yuan et al. [66] proposed a local DM sub-halo scenario to explain the tentative peak structure at 1.4 TeV in the electron and positron spectrum of DAMPE. In this subsection we examine whether a box-shaped electron/positron spectrum can reasonably reproduce the data. Since the propagation of the electrons and positrons is usually expected to be independent of the initial spectrum, we take the parameters of the distance and the mass of the hypothesized subhalo as 0.1 kpc and $1.9 \times 10^7\ M_\odot$, the same as those of [66]. We show our likelihood map in Fig.5 with the mass ratio $m_\phi/m_{\rm DM} = 0.995$ and $m_\phi/m_{\rm DM} = 0.5$. And in Fig.6, we plot the best fit result for $m_\phi/m_{\rm DM} = 0.995$, $m_{\rm DM} = 3000$ GeV and $\langle\sigma v\rangle = 1.44 \times 10^{-26}$ cm^3 s^{-1}. In order to explain the tentative peak structure of DAMPE data at 1.4 TeV, we need a high mass ratio of $\gtrsim 0.995$, which almost leads to a line spectrum that is un-distinguishable from normal scenario without the intermediates.

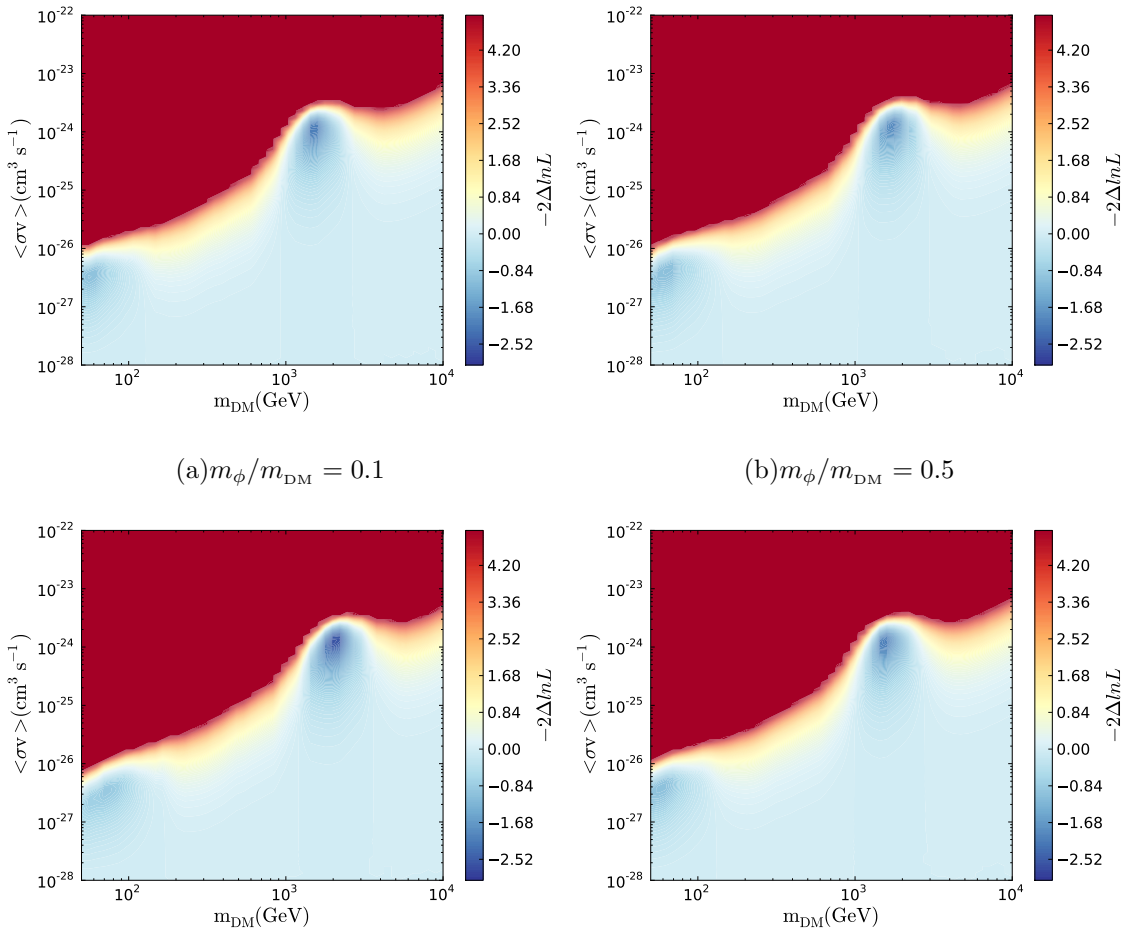

(a)$m_\phi/m_{\rm DM} = 0.1$ (b)$m_\phi/m_{\rm DM} = 0.5$

(c)$m_\phi/m_{\rm DM} = 0.9$ (d)PPPC4

FIG. 3: Likelihood map of different mass ratio ($m_\phi/m_{\rm DM} = 0.1,\ 0.5,\ 0.9$) and PPPC4 on $m_{\rm DM}$ and $<\sigma v>$ plane based on the AMS-02 and DAMPE data where $-2\Delta\ln\mathcal{L} = -2\left(\ln\mathcal{L} - \ln\mathcal{L}_0\right)$ and $\mathcal{L}_0$ is the likelihood without DM contribution.

IV. CONCLUSION

In this work, we use the AMS-02 and DAMPE data to search for possible DM annihilation signal from a class of models with two-step annihilation process including intermediate scalar particles. The resulting electron/positron spectrum from such DM models looks like a box shape, and may be imprinted in high energy resolution spectra of cosmic ray electrons/positrons (by e.g., DAMPE).

We do not find any significant annihilation signal with such box-shaped spectrum. The 95% upper limits of the DM annihilation cross section range from $\sim 10^{-26}$ cm^3/s to $\sim 10^{-24}$ cm^3/s for the DM particle mass between 50 GeV and 10 TeV. A 2 TeV DM component

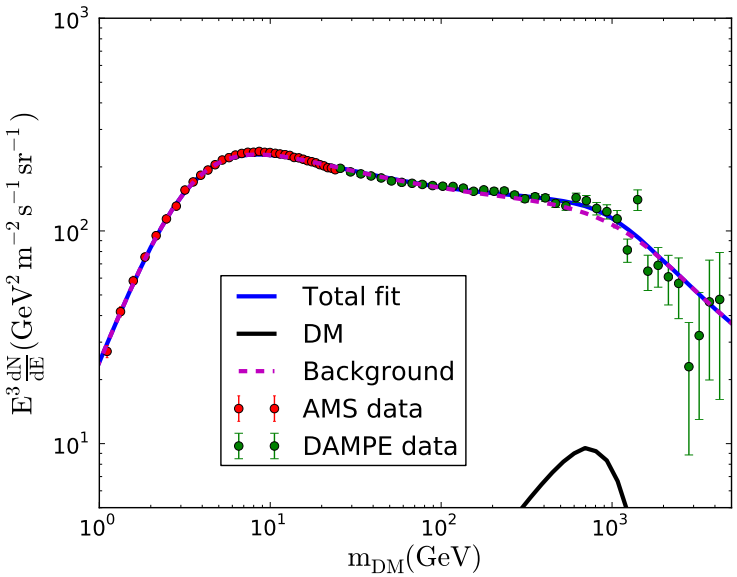

FIG. 4: The model prediction of energy spectrum of electrons/positrons with the best-fit parameters, $m_{\rm DM} = 1.96$ TeV, $\langle \sigma v \rangle = 1.32 \times 10^{-24}$ cm^3/s, and $m_\phi/m_{\rm DM} = 0.9$, compared with the data from AMS-02 [19] and DAMPE [56].

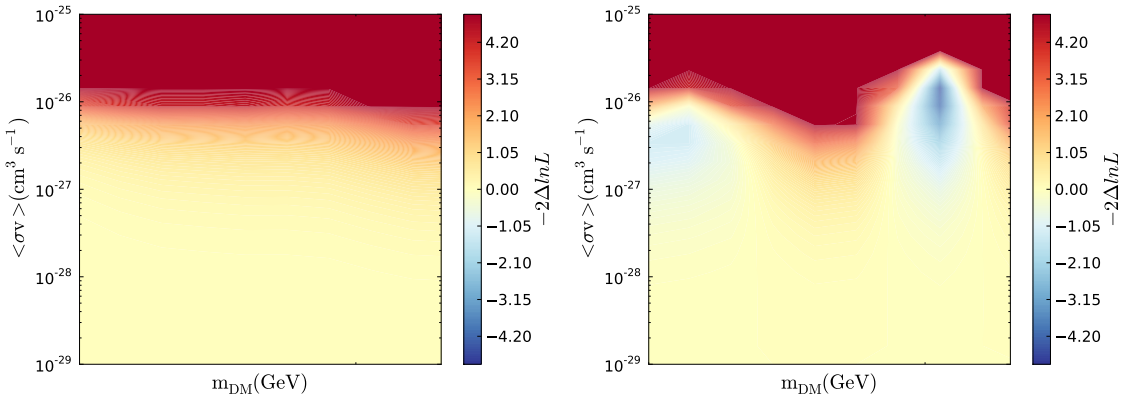

(a)$m_\phi/m_{\rm DM} = 0.5$ (b)$m_\phi/m_{\rm DM} = 0.995$

FIG. 5: Likelihood map of mass ratio $m_\phi/m_{\rm DM} = 0.5,\ 0.995$ on $m_{\rm DM}$ and $\langle \sigma v \rangle$ plane with a local (0.1kpc) DM subhalo ($1.9 \times 10^7\ M_\odot$).

is found to improve slightly the fit to the DAMPE data around 700 GeV, but the significance is very low. With a local DM subhalo, as assumed in [66], we find out that a high mass ratio (for which the resulting spectrum is line like) can improve the fit. In view of the narrow energy range of the tentative peak at 1.4 TeV, such a result is actually anticipated. Future measurements of the fine structures of the electrons/positrons with higher precision may

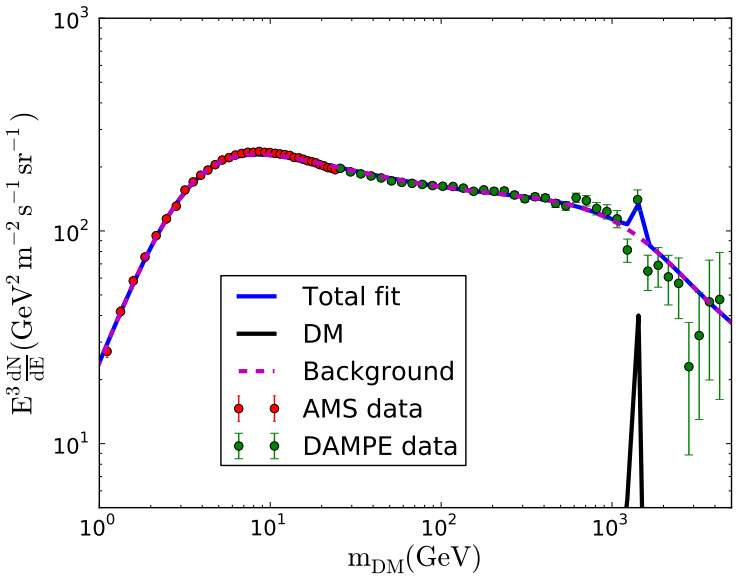

FIG. 6: The same as Fig.4 but with a local DM subhalo. $m_\phi/m_{\rm DM} = 0.995$, $m_{\rm DM} = 3$ TeV and $\langle\sigma v\rangle = 1.44 \times 10^{-26}$ cm^3/s with the distance and mass of subhalo as 0.1 kpc and 1.9×10^7 $M_\odot$[66].

shed new light on the indirect detection of DM with characteristic spectral features.

Acknowledgments

This work is supported by the National Key Research and Development Program of China (No. 2016YFA0400200), National Natural Science of China (Nos. 11722328, 11773075, U1738206, U1738210), the Youth Innovation Promotion Association of Chinese Academy of Sciences (No. 2016288), the Natural Science Foundation of Jiangsu Province (No. BK20151608), and the 100 Talents program of Chinese Academy of Sciences.

[1] P. J. Fox, R. Harnik, J. Kopp, and Y. Tsai, Phys. Rev. D **85**, 056011 (2012), 1109.4398.

[2] J. Goodman, et al., Phys. Rev. D **82**, 116010 (2010), 1008.1783.

[3] D. S. Akerib et al., Phys. Rev. Lett. **112**, 091303 (2014), 1310.8214.

[4] J. Angle et al., Phys. Rev. Lett. **100**, 021303 (2008), 0706.0039.

[5] J. L. Feng, K. T. Matchev, and F. Wilczek, Phys. Rev. D **63**, 045024 (2001), astro-ph/0008115.

[6] M. Ackermann et al., Phys. Rev. Lett. **107**, 241302 (2011), 1108.3546.

[7] O. Adriani et al., Phys. Rev. Lett. **106**, 201101 (2011), 1103.2880.

[8] M. Ackermann et al., Phys. Rev. Lett. **108** 011103 (2012), 1109.0521.

[9] A. A. Abdo et al., Phys. Rev. Lett. **102**, 181101 (2009), 0905.0025.

[10] M. Aguilar et al., Phys. Rev. Lett. **110**, 141102 (2013).

[11] G. Bertone, D. Hooper and J. Silk, Phys. Rept. **405**, 279 (2005), hep-ph/0404175.

[12] L. Bergstrom, Rept. Prog. Phys. **63**, 793 (2000).

[13] G. Bertone, Particle dark matter: Observations, models and searches, Cambridge University Press, Cambridge (2010).

[14] L. Bergstrom, arXiv:1202.1170 (2012).

[15] O. Adriani et al., Nature **458**, 607 (2009), 0810.4995.

[16] M. Aguilar et al., Phys. Rev. Lett. **110**, 141102 (2013).

[17] L. Accardo et al., Phys. Rev. Lett. **113**, 121101 (2014).

[18] J. Chang et al., Nature **456**, 362 (2008).

[19] M. Aguilar et al., Phys. Rev. Lett. **113**, 221102 (2014).

[20] O. Adriani et al., Phys. Rev. Lett. **102**, 051101 (2009), 0810.4994.

[21] O. Adriani, et al., Phys. Rev. Lett. **105**, 121101 (2010), 1007.0821.

[22] M. Aguilar et al., Phys. Rev. Lett. **117**, 091103 (2016).

[23] M.-Y. Cui, Q. Yuan, Y.-L. S. Tsai, and Y.-Z. Fan, Phys. Rev. Lett. **118**, 191101 (2017), 1610.03840.

[24] A. Cuoco, M. Kramer, and M. Korsmeier, Phys. Rev. Lett. **118**, 191102 (2017), 1610.03071.

[25] L. Bergström, T. Bringmann, and J. Edsjö, Phys. Rev. D **78**, 103520 (2008), 0808.3725.

[26] V. Barger, W.-Y. Keung, D. Marfatia, and G. Shaughnessy, Phys. Lett. B **672**, 141 (2009), 0809.0162.

[27] M. Cirelli, M. Kadastik, M. Raidal, and A. Strumia, Nucl. Phys. B **813**, 1 (2009), 0809.2409. [Addendum-ibid. **873**, 530 (2013)]

[28] P.-F. Yin, Q. Yuan, J. Liu, J. Zhang, X.-J. Bi, S.-H. Zhu, and X. Zhang, Phys. Rev. D **79**, 023512 (2009), 0811.0176.

[29] J. Zhang, X.-J. Bi, J. Liu, S.-M. Liu, P.-F. Yin, Q. Yuan, and S.-H. Zhu, Phys. Rev. D **80**, 023007 (2009), 0812.0522.

[30] L. Feng, R.-Z. Yang, H.-N. He, T.-K. Dong, Y.-Z. Fan, and J. Chang, Phys. Lett. B **728**, 250 (2014), 1303.0530.

[31] Q. Yuan, X.-J. Bi, G.-M. Chen, Y.-Q. Guo, S.-J. Lin and X. Zhang, Astropart. Phys. **60**, 1 (2015), 1304.1482.

[32] J. Kopp, Phys. Rev. D **88**, 076013 (2013), 1304.1184.

[33] I. Cholis and D. Hooper, Phys. Rev. D **88**, 023013 (2013), 1304.1840.

[34] H.-B. Jin, Y.-L. Wu and Y.-F. Zhou, J. Cosmol. Astropart. Phys. **11**, 026 (2013), 1304.1997.

[35] H. Yüksel, M. D. Kistler, and T. Stanev, Phys. Rev. Lett. **103**, 051101 (2009), 0810.2784.

[36] D. Hooper, P. Blasi, and P. Dario Serpico, J. Cosmol. Astropart. Phys. **01**, 025 (2009), 0810.1527.

[37] S. Profumo, Central European Journal of Physics **10**, 1 (2012), 0812.4457.

[38] D. Malyshev, I. Cholis, and J. Gelfand, Phys. Rev. D **80**, 063005 (2009), 0903.1310.

[39] H.-B. Hu, Q. Yuan, B. Wang, C. Fan, J.-L. Zhang, and X.-J. Bi, Astrophys. J. Lett. **700**, L170 (2009), 0901.1520.

[40] P. Blasi, Phys. Rev. Lett. **103**, 051104 (2009), 0903.2794.

[41] T. Linden and S. Profumo, Astrophys. J. **772**, 18 (2013), 1304.1791.

[42] P.-F. Yin, Z.-H. Yu, Q. Yuan, X.-J. Bi, Phys. Rev. D **88**, 023001 (2013), 1304.4128.

[43] Nima Arkani-Hamed, Douglas P. Finkbeiner, Tracy R. Slatyer, Neal Weiner Phys.Rev.D79:015014,2009

[44] A. Lopez, C. Savage, D. Spolyar, and D. Q. Adams, J. Cosmol. Astropart. Phys. **03**, 033 (2016), 1501.01618.

[45] A. Scaffidi, K. Freese, J. Li, C. Savage, M. White, and A. G. Williams, Phys. Rev. D **93**, 115024 (2016), 1604.00744.

[46] M. Papucci and A. Strumia, J. Cosmol. Astropart. Phys. **03**, 014 (2010), 0912.0742.

[47] G. Bertone, M. Cirelli, A. Strumia, and M. Taoso, J. Cosmol. Astropart. Phys. **03**, 009 (2009), 0811.3744.

[48] L. Bergstrom, G. Bertone, T. Bringmann, J. Edsjo, and M. Taoso, Phys. Rev. D **79**, 081303 (2009), 0812.3895.

[49] T. R. Slatyer, N. Padmanabhan, D. P. Finkbeiner, Phys. Rev. D **80**, 043526 (2009), 0906.1197.

[50] T. R. Slatyer, Phys. Rev. D **93**, 023527 (2016), 1506.03811.

[51] J. Mardon, Y. Nomura, D. Stolarski, and J. Thaler, J. Cosmol. Astropart. Phys. **05**, 016 (2009), 0901.2926.

[52] G. Elor, N. L. Rodd, and T. R. Slatyer, Phys. Rev. D **91**, 103531 (2015), 1503.01773.

[53] X.-J. Huang, C.-C. Wei, Y.-L. Wu, W.-H. Zhang, and Y.-F. Zhou, Phys. Rev. D **95**, 063021 (2017), 1611.01983.

[54] A. Ibarra, S. L. Gehler and M. Pato, J. Cosmol. Astropart. Phys. **07**, 043 (2012), 1205.0007.

[55] S. Li et al., submitted (2017).

[56] G. Ambrosia et al., doi:10.1038/nature24475 (2017).

[57] J. Chang, Chinese Journal of Space Science **34**, 550 (2014).

[58] J. Chang et al., Astropart. Phys. **95**, 6 (2017), 1706.08453.

[59] M. Cirelli, G. Corcella, A. Hektor, G. Hutsi, M. Kadastik, P. Panci, M. Raidal, F. Sala, and A. Strumia, J. Cosmol. Astropart. Phys. **03**, 051 (2011), 1012.4515.

[60] T. Sjostrand, S. Mrenna and P. Z. Skands, Comput. Phys. Commun. **178**, 852 (2008), 0710.3820.

[61] A. W. Strong and I. V. Moskalenko, Astrophys. J. **509**, 212 (1998), astro-ph/9807150.

[62] C. Evoli, D. Gaggero, D. Grasso and L. Maccione, J. Cosmol. Astropart. Phys. **10**, 018 (2008), 0807.4730.

[63] X. Huang, Y.-L. S. Tsai, and Q. Yuan, Comput. Phys. Commun. **213**, 252 (2017), 1603.07119.

[64] J. N. Bahcall, R. M. Soneira, Astrophys. J. Suppl., **44**, 73 (1980).

[65] T. Kamae, et al., Astrophys. J., **647**, 692 (2006).

[66] Q. Yuan et al., submitted (2017).